Resilient Housing and Climate Change: Analysis of Ozone Spatial Variations Based on Experimentally Validated CFD Simulations

Qi Zhang[1,2,3], Linxue Li[1], William W. Braham[2], Nan Ma[3,4,*]
[1]College of Architecture and Urban Planning, Tongji University, Shanghai 200092, China
[2]Department of Architecture, University of Pennsylvania, Philadelphia, PA 19104, United States
[3]Laboratory for Healthy, Environmental, and Resilient Buildings, Worcester Polytechnic Institute, Worcester, MA 01609, United States
[4]Department of Civil, Environmental, & Architectural Engineering, Worcester Polytechnic Institute, Worcester, MA 01609, United States

Abstract

Ozone has been linked to both acute and chronic health effects, and with the ongoing trend of global warming, the associated health risks are expected to increase. Our study focuses on investigating the spatial variations of ozone in typical rowhouses in one of the most ozone-polluted cities in the United States, using experimentally validated computational fluid dynamics (CFD) simulations. Our results indicate that houses facing south-east and south-west have significantly higher mean ozone concentrations, with higher concentrations observed on upper floors. We also found that indoor ozone exposure at 1.0m height could pose a significant risk to children's health.

Highlights

- The CFD models were calibrated and validated based on in-field measurements
- Future trends of indoor ozone exposures under global warming scenarios were simulated using validated CFD models
- Corresponding architectural solutions were proposed for reducing indoor health risks

Introduction

The Global Burden of Diseases, Injuries, and Risk Factors Study 2015 (GBD 2015) identified air pollution as a significant contributor to the global disease burden, with ozone being one of the most widely recognized ambient air pollutants that cause both acute and chronic health effects (Cohen et al., 2017; World Health Organization, 2021; Bell et al., 2007). Ozone exposure was ranked as the 34th-leading mortality risk factor in GBD 2015, leading to 254,000 deaths and contributing to an estimated 8.0% of global lung cancer and chronic obstructive pulmonary disease (COPD) mortality (Cohen et al., 2017; Dockery & Evans, 2017). Studies have shown that long-term exposure to ozone is associated with respiratory problems such as cough, chest pain, decreased pulmonary function, and increased asthma incidence (Jan et al., 2017; Levy et al., 2001; Mudway & Kelly, 2000). Furthermore, trisks to public health are expected to worsen as the climate warms because higher temperature accelerates ozone formation (Chang et al., 2014; Westervelt et al., 2016).

In urban environments, building occupants spend most of their time indoors (Klepeis et al., 2001), where they can be exposed to outdoor pollution that infiltrates indoor spaces via natural ventilation (Chen et al., 2012; Weschler, 2000). This exposure could be further compounded by the transport of ozone from the outdoor environment to the indoor enviornment through air exchange of windows, degrading the indoor air quality (IAQ) (Sundell et al., 2011a). Since indoor ozone mainly originates from outdoor sources, proper building design (e.g., building geometry, envelope, window configuration) is critical in preventing outdoor ozone penetration and aiding in the dilution of indoor ozone (Ma et al., 2021). In this case, residential houses without mechanical ventilation systems are particularly vulnerable to ozone pollution, making it essential to explore optimal design approaches for healthy residential dwelling. Moreover, windows of residential house are operable, making them ideal for using natural ventilation to improve IAQ. Therefore, investigating optimal design approaches for ozone mitigation in residential houses is of significant importance.

However, IAQ has received limited attention as part of building design objectives, with architects typically prioritizing aesthetics, daylighting (Wong, 2017), thermal comfort (Alizadeh & Sadrameli, 2018), and energy saving (Mackay & Probert, 2000) over IAQ (Sloan Brittain et al., 2021). To this end, healthy buildings have to rely on heating, ventilating, and air conditioning (HVAC) systems, which are typically added in the later stages of the design process to modify air characteristics. Unfortunately, incorporating architectural solutions for delivering healthy air into the building's initial design is currently overlooked. This is a significant issue, as some occupants may not afford air conditioners and some buildings may have air conditioning systems that become less efficient over time. With more frequent blackouts and longer durations, relying solely on active systems such as HVAC and air purifiers is becoming increasingly difficult. To address these challenges, it is crucial to prioritize passive building performance to reduce reliance on these active systems. This entails linking building design (e.g., building geometry and window configuration) with IAQ during the design phase. One effective approach is through computer fluid dynamics (CFD), which combines numerical methods and pollutant concentration visualization to improve IAQ management in buildings. By prioritizing IAQ alongside other design objectives, it will not only improve occupant well-being but also contribute to sustainable and resilient building practices (Ma et al., 2023).

https://doi.org/10.26868/25222708.2023.1472

Accoding to the American Lung Association's 2020 State of the Air report, the Philadelphia-Reading-Camden area (also known as the greater Philadelphia area) has unhealthy levels of outdoor ozone and the city of Philadelphia is ranked among the nation's 25 worst ozone-polluted cities (American Lung Association, 2020). Rowhouses are the dominant housing type in Philadelphia due to their space-efficiency and cost-effectiveness, characterized by the narrow street frontage and attached adjacent houses on both sides (Schade & Architects, 2008). This architectural configuration makes rowhouses particularly susceptible to pollutants from the street which can substantially affect IAQ through the building's street-facing surface and windows. To address these challenges, our study focuses on investigating the spatial variations of indoor ozone under global warming senarios and reveal future trends of indoor ozone exposures by using experimentally-validated CFD models. Specifically, we executed RhinoCFD which is a CFD software plugin built directly into the Rhino environment and powered by CHAM's PHOENICS. It allows us to effectively simulate the spatial variations of indoor ozone concentrations in order to reveal the impacts of different building geometry, window configuration, and design interventions. Ultimately, our study aims to develope the architectual strategies and interventions that can mitigate indoor ozone pollution and contribute to improving IAQ in rowhouses.

Related Work

Among the existing studies, ventilation rate has been widely used to evaluate IAQ performance and is included as one of the methods for managing IAQ in 55 green building programs of 31 worldwide certifications (Wei et al., 2015). Increasing ventilation rate generally beneficial for improving IAQ and human health, particularly when the primary source of pollution is indoors (Sundell et al., 2011b). However, as ozone is an oudoor pollutant that infiltrates residential houses, ventilation rate may not be sufficient to refelct ozone concentrations. In Ben-David and Waring's study (Ben-David & Waring, 2016), they used simulated ventilation rates to estimate IAQ and found that higher ventilation rates may not be representative of the specific level of air pollutants. This finding underscores the limitations of using ventilation rates alone as a reliable indicator of ozone concentrations in residential environments.

Prior research has primarily examined the impact of increased ventilation on indoor ozone concentrations, but it has focused predominantly on mechanical systems rather than building design. For exmaple, Walker and Sherman (Walker & Sherman, 2013) investigated the effect of ventilation system on indoor ozone levels under two modes of operation - continuous exhaust and intermittent exhaust - and found that shutting down ventilation systems during periods of high outdoor ozone levels could significantly reduce indoor ozone levels. Ben-David and Waring (Ben-David & Waring, 2018) looked into the effects of ventilation and filtration on building exposure to ozone in a typical office with mechanical systems to explore the impact of ventilation on pollutant concentrations. Lai et al. (Lai et al., 2015) reported on the relationship between ventilation and indoor/outdoor ozone concentration by measuring ventilation rates and ozone concentration under different mechanical ventilation systems. While all of these studies shed light on the impact of mechanical systems on IAQ, they did not delve into the importance of the building design itself.

The literature contains only a limited number of studies that explore the relationship between building design and IAQ. For example, Ma et al. (Ma et al., 2022) conducted a preliminary investigation into the impact of building envelope design variables on preventing the infiltration of outdoor ozone into indoor spaces. Their findings indicate that appropriate architectural design can help mitigate penetration trends. However, the study was limited to only four houses in the urban Philadelphia area. Further research with a larger number of sample size is needed to fully understand the relationship between building design and indoor ozone concentrations. One approach to address this is to use experimentally-validated CFD models. CFD software allows for the representation of the original and continuous physics quantity field in time and space through a series of finite discrete points with variable values, which is an improvement compared to single-point measurements from actual experiments. However, it is important to validate CFD models using experimental data to calibrate numerical and modeling errors and to provide accurate trends of pollutant concentrations.

Therefore, the primary obejective of this study is to investigate the risks associated with indoor ozone exposure in the most representative scenarios under climate change and examine how building design variables can contribute to mitigating outdoor ozone pollution, using validated CFD models based on the on-site measurement.

Field Survey and Measurement Campaign

Overview of rowhouses in Philadelphia

A dominant type of rowhouse design was selected as the case study, characterized by rectangular floor plans and straight and rectangular facades. The specific rowhouse chosen for on-site measurements and CFD model validation is located in the Philadelphia's limited traffic zone, was constructed in 1935, and has not undergone any major renovations or refurbishments (Figure 1).

Figure 1: Location of the case study rowhouse.

Indoor ozone concentrations were measured in a room with dimensions of 4.15×3.80×3.00 m and a length-to-

https://doi.org/10.26868/25222708.2023.1472

width ratio of 1.09. The exterior wall facing the street is made of brick and has an area of 12.47 m^2, with a window perimeter of 10.18 m, a length-to-width ratio of 1.624, and a window-to-wall ratio of 0.222.

On-site monitoring campaigns

It is important to consider occupant behavior when modeling IAQ, as it can introduce uncertainties in building performance. In this study, data were collected during the normal use period by the residents over a period of 12 days from August 17th to August 29th, 2020. The occupants were asked to record the daily window opening times. According to the records, the windows remained closed through the entire monitoring period. No significant sources of ozone, such as photocopiers or printers, were found in the room studied.

Hourly outdoor ozone data were obtained from the U.S. Environmental Protection Agency (EPA)'s AirNow web application (https://www.airnow.gov). The study area had only one monitoring site for ozone within a reasonable distance (within 10 km). Outdoor climate conditions were monitored every 5 minutes by a HOBO RX3000 weather station (Onset Computer Corporation, Bourne, MA, USA), which was set up on a building rooftop and reported outdoor air temperature, relative humidity, wind speed, and solar radiation. The meteorological stations are provided in Figure1. Indoor ozone was measured at 1-minute intervals using a UV-absorbance ozone analyzer (Model 202, 2B Technologies Inc., Boulder, CO, USA) that measures concentrations between 0 and 250 ppm by the principle of UV absorption at 254 nm. The sampling resolution is 0.1 ppb, and the accuracy is either 1.5 ppb or 2% of the reading whichever is greater.

Tracer gas experiments

The CO_2 tracer gas experiment was performered to determine the infiltration rate of the building envelope, including the walls and windows, providing evidence for calibrating and validating the porosity in the RhinoCFD setup. The experiment was conducted in the test rowhouse with all windows and doors closed. During this process, CO_2 was released from a regulator connected to a compressed CO_2 cylinder (~25 kg full) until the indoor CO_2 concentration measured 2500 ppm, at which point the valve to the cylinder was closed. Next, a fan was turned on for 5 min to mix the air in the space, ensuring a consistent CO_2 concentration through the indoor air. The indoor CO_2 concentration was continuously recorded every minute using a Telaire 7001 CO_2 monitor connected to an Onset HOBO U12 data-logger. The experiment was concluded when the CO_2 concentration stepped down at about the same background level (less than 700 ppm). The tracer gas analysis relies on describing the overall shape of the decay curve. According to the American Society for Testing and Materials (ASTM) E741 standard, one way to estimate the infiltration rate is to fit a curve to the logarithmic form of CO_2 concentration (Y) against time (X) and determine the constants b_0 and b_1 in the relationship as given by equation (1).

$$Y = b_0 + b_1 X \quad (1)$$

As the estimators b_0 and b_1 may not be either direct or exact measurement results, the mean squared error (MSE) was computed to measure the propagation of error using equation (2).

$$MSE_N = \frac{1}{n-2} \sum_{t=0}^{i} (Y_i - \hat{Y}_i)^2 \quad (2)$$

where Y_i is the natural logarithm of the measured CO_2 concentration at time i, and $\hat{Y}_i$ is the natural logarithm of the approximated CO_2 concentration at time I, using b_0 and b_1 as predictors. n is the number of CO_2 readings collected during the entire tracer gas test.

CFD Modelling and Validation

CFD modeling and simulation settings

We performed the CFD simulation using RhinoCFD (version 2.1.2), which is a CFD software plugin integrated directly into the Rhino environment and powered by CHAM's PHOENICS. The simulation settings are explained in the following sections.

Model. A 3D model was created to simulate the real conditions of the selected rowhouse, including the indoor furniture that is likely to affect the airflow pattern, as depicted in Figure 2. The envelope facing the street along with the window, was simplified as one object, defined as the Plate with a specific porosity, allowing air and pollutants to pass through. The other surfaces, such as the remaining walls, ceiling, floor, and furniture, were set with non-slip and adiabatic boundary conditions.

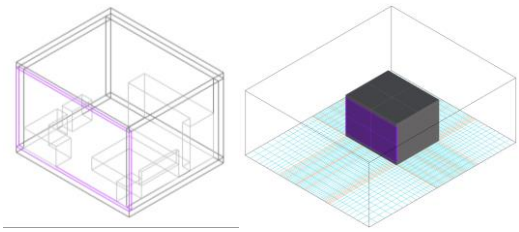

Figure 2: RhinoCFD simulation model.

Computational mesh. RhinoCFD utilizes a cut-cell method called PARSOL to automatically identify the solid and fluid parts of each cell and applies the appropriate boundary conditions. This results in the computational mesh consisting of rectangular cells, totaling approximately 190,000 ($63 \times 74 \times 41$). We employed an uneven mesh density, with higher resolution near the objects and lower density further away. This approach ensures both calculation accuracy and faster processing times.

Domain. A 3D rectangular Cartesian region was created to predict airflow patterns and temperature distributions in buildings, as well as wind flows around buildings. The domain's space is filled with gases, and air is modeled as compressible using the ideal-gas law. The outdoor climate parameters used in CFD simulation environment are based on field measurements and represent the 75th percentile data for Philadelphia, which represents the dominant data for the city (Table 1). The wind direction was directly retrieved from the TMYs file. In this study, daytime refers to 8:00 - 20:00, and nighttime refers to 20:00 - 8:00. The ambient temperature in the simulation

https://doi.org/10.26868/25222708.2023.1472

is set to 32 ℃ during daytime and 20 ℃ during nighttime. The direct and diffuse solar radiation during the day are set to 300 W/m2 and 50 W/m2, respectively. The direct and diffuse solar radiation at night are set to 1 W/m2. The wind direction is 225° with a velocity of 1.5 m/s.

Pollutants model. To simulate the transmission and distribution of ozone indoors and outdoors, a pollutant model was established with a molecular weight of 47.998 g/mol (Yang & Zhao, 2023). In this model, ozone is set to be carried by the wind, entering the room from outside with the airflow. According to our field measurements, we identified the most frequently occurred concentration levels and reported them in Table 1, in order to investigate the indoor ozone exposure under most typical conditions. Specifically, the outdoor ozone concentration is set to 40 ppb during the day and 16 ppb at night.

Table 1: Model fixed parameters settings.

Item	Description	Value
Climate	External temperature - daytime	32 ℃
	External temperature - nighttime	20 ℃
	Direct solar radiation - daytime	300 W/m2
	Direct solar radiation - nighttime	1 W/m2
	Diffuse solar radiation - daytime	50 W/m2
	Diffuse solar radiation - nighttime	1 W/m2
	External wind direction	225 °
	External wind velocity	1.5 m/s
Pollutant	External ozone concentration - daytime	40 ppb
	External ozone concentration - nighttime	16 ppb

Turbulence model. The Chen-Kim modified k-ε turbulence model was used in this study, which is capable of characterizing the various dynamic processes occurring in turbulent flows. Chen-Kim's improvement of the two-equation k-epsilon model provides better prediction of separation and vortices than the classic k-epsilon. In this model, global residuals are normalized for assessing convergence, with a maximum thresholds of and 10-5 for normalized residual and 1% for error valuse percentages. Specifically, the solution is considered convergent when the normalized residuals fall below 10-5 and the error values percentage fell below 1% for all variables.

Transient model. Most previous studies have used steady-state models to simulate the general airflow pattern under steady-state conditions. However, a single steady-state model may not accurately capture the transient and complex airflows. In this study, the airflow is assumed to be transient and compressible. The simulation runtime is set to 10 minutes, allowing sufficient time for the ozone concentration to reach the most common values measured in the studied rowhouse. The time step frequency is set to 30 seconds for 20 steps, and 50 iterations are set to converge each time step. In total, the simulation runs for 1,000 iterations to ensure an acceptable level of accuracy and computational time.

CFD model validation

To ensure the accuracy and reliability of a CFD model, it is essential to validate it with data obtained from empirical models and/or measurements in the real environment (Hajdukiewicz et al., 2013). In this study, some parameter settings for the CFD model, such as temperature, solar radiation, wind velocity, and outdoor ozone concentration, were determined from field measurements (Table 1). However, other parameters presented in Table 2, including the porosity of envelope and the simulation runtime, require calibration and validation. These parameters have a certain range, and our validation process aims to set a series of models by adjusting the parameters values within the range. Through performing multiple simulations and comparing the results with the underlying mechanism of the field measurements (i.e., indoor ozone concentrations), the proper settings were determined. This validation process evaluates the reliability of the CFD model, enabling its use for further analyses and predictions.

The root mean square deviation (RMSD) given in Equation (3) was used to support the calibration procedures. RMSD provides a comprehensive measure of the deviation between simulated data and measured data, expressed as a single number. Previous studies have made seminal contributions using these criteria, which have been proven effective for obtaining accurate results (Kamel et al., 2021; Xu et al., 2022).

$$RMSD\ (u, w) = \sqrt{\frac{1}{n}\sum_{i=1}^{n}((u_1 - w_1)^2 + (u_2 - w_2)^2 + \cdots + (u_n - w_n)^2)} \quad (3)$$

where u is the data outputs of RhinoCFD simulations and w is the on-site measured data.

Table 2: Model validated parameters and ranges.

Item	Description	Value
Envelop	Porosity of the external wall	0.01 - 0.99
Time	Simulation runtime	0 - 10 min

Validated CFD for twelve simulated rowhouses

To reveal spatial variations of ozone levels across the city under future climate change, we carefully selected 12 typical rowhouses located in three blocks. Based on the validated parameter settings (Figure 3), RhinoCFD models were established for each of these rowhouses. The selected rowhouses present diverse building design characteristics, including geometry and orientation, as summarized in Table 3. We simulated the indoor ozone concentrations during daytime for each of these 12 rowhouses, assuming an outdoor ozone concentration of 100 ppb under the future climate change scenario. The objective was to analyze the spatial variations of residential ozone concentrations and to explore potential design interventions.

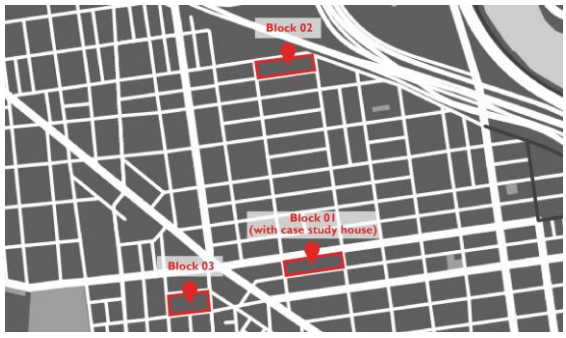

Figure 3: Location of simulated 12 rowhouses.

Table 3: Design variables value for 12 rowhouses.

https://doi.org/10.26868/25222708.2023.1472

Building	Width (m)	Length (m)	Height (m)	Floor height (m)	Orientation
01	6.3	18.0	9.9	3.3	SE
02	6.9	12.8	9.9	3.3	SW
03	4.8	16.0	7.0	3.5	NW
04	6.6	12.8	10.8	3.6	NE
05	6.9	14.4	7.0	3.5	SE
06	5.7	16.8	7.0	3.5	SW
07	5.4	16.8	7.0	3.5	NW
08	6.0	18.0	10.5	3.5	NE
09	6.4	19.6	12.0	4.0	SE
10	6.4	19.6	12.0	4.0	SW
11	6.4	19.6	8.0	4.0	NW
12	6.4	19.6	12.0	4.0	NE
Building	**Length/ Width**	**Wall surface area** (m2)	**Floor wall surface area** (m2)	**Floor area** (m2)	
01	2.10	62.37	20.79	113.40	
02	1.86	68.31	22.77	88.32	
03	3.33	33.60	16.80	76.80	
04	1.94	71.28	23.76	84.48	
05	2.09	48.30	24.15	99.36	
06	2.95	39.90	19.95	95.76	
07	3.11	37.80	18.90	90.72	
08	3.00	63.00	21.00	108.00	
09	3.06	76.80	25.60	125.44	
10	3.06	76.80	25.60	125.44	
11	3.06	76.80	25.60	125.44	
12	3.06	76.80	25.60	125.44	

Results and Discussion

Tracer gas test results

The decay of CO_2 back to ambient levels was measured over several hours after controlled release of CO_2 in the study rowhouse. According to the ASTM E741 standard, indoor CO_2 concentrations predictably follow an exponential decay curve over time, with the natural logarithm being alomost linear. The best linear fit was derived. The results of the linear model fit show a fairly good fit with a value of 0.894 for R-squared and a value of 0.011 for MSE. The infiltration rate of the test building was 0.4390/h. The resulting infiltration rate is for the whole building envelope, including walls and windows, which provides evidence for the calibration and validation of porosity in the CFD simulation setup.

Validation of numerical simulation results

Table 4 presents the indoor ozone concentrations measured over a period of 12 consecutive days, with average values of 23.00 ppb during daytime and 11.07 ppb during nighttime. In oder to evaluate the consistency between the simulated and measured data, we obtained simulated indoor ozone concentrations at 30-second intervals for different porosity cases during the first 10 minutes. We used RMSD as the evaluation metric. Our fundings indicate that the simulated data match the measured data best when the porosity is set to 0.18 and the simulation runtime is 4 minutes and 30 seconds, with an RMSD value of 1.06, which falls within the acceptable error range outline in ASHRAE's Guideline 14-2014.

Table 4: The RMSD results of the validated model.

Items	Unit	Measured data	Simulated data
Ozone daytime	(ppb)	23.00	21.18
Ozone nighttime	(ppb)	11.07	11.98
RMSD		**1.06**	

Simulation results for twelve rawhouses under climate change

The indoor ozone concentration distributions in 12 typical rowhouses were simulated using RhinoCFD, with an outdoor ozone concentration of 100 ppb during daytime. Three-dimensional ozone concentration data were collected within the building boundary conditions. We extracted and exported ozone concentration data for each floor of every building at three heights: 1.0m, 1.5m, and 1.7m. These heights correspond to the standing height of children (sitting height for adults), the standing height of female adults, and standing height of male adults, respectively. The data were then visualized and analyzed for the further insights.

Figure 4 illustrates the distribution of indoor ozone concentrations at a height of 1.5m per floor for 12 rowhouses, revealing significant differences between houses with different orientations. Specifically, houses facing south-west and south-east exhibited much higher concentrations than those facing north-west and north-east. Furthermore, houses with the same orientation displayed similar trends in ozone distribution, but exhibited some variability in concentrations due to differences in geometry, such as length-to-width ratio. Additionally, the indoor ozone concentration exhibited a certain gradient difference on different floors, increasing with the number of floors in buildings facing south-west and south-east and showing the opposite pattern in buildings facing north-west and north-east.

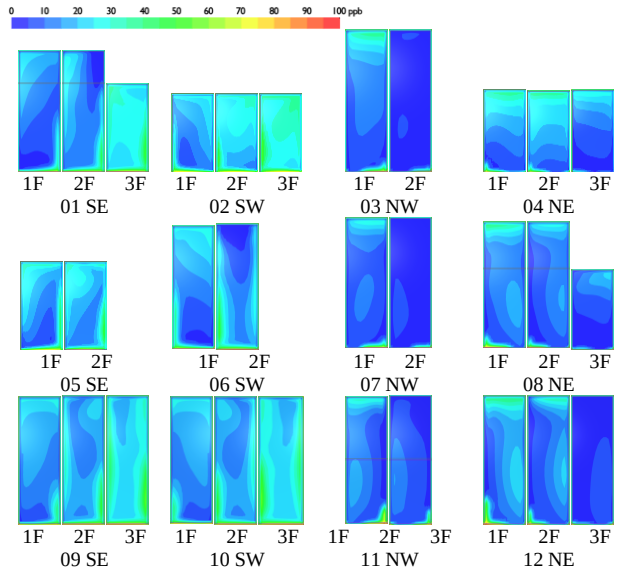

Figure 4: Indoor ozone concentration distribution at 1.5m height per floor of 12 rowhouses.

Orientation analysis. Analysis of building orientation revealed a clear relationship with indoor ozone concentrations, as shown in Table 5. The mean ozone concentration in houses facing south-east (25.74 ppb) was similar to that in houses facing south-west (23.68 ppb), while those facing north-west and north-east had lower mean ozone concentrations of 13.62 ppb and 17.18 ppb, respectively. These findings indicate that houses facing south-east and south-west have significantly higher mean ozone concentrations compared to those facing north-

west and north-east. This relationship can be attributed to the prevailing winds in Philadelphia, which bring more ambient ozone into buildings on the windward side. In addition, strong solar radiation and higher temperatures in the southern direction accelerate ozone production.

Table 5: Summary statistics of indoor ozone concentration in rowhouses with different orientation.

Orientation	Mean±SD	Min	Median	95th Percentile	Max
SE	25.74±12.83	0.03	24.63	52.90	87.37
SW	23.68±13.90	0.00	20.89	47.59	87.40
NW	13.62±12.93	0.00	9.38	40.00	84.23
NE	17.18±12.43	0.00	13.34	40.00	87.37

Ozone exposures at different floor levels. Figure 5 illustratess the indoor ozone concentration distribution on each floor for four different orientations, highlighting the concentration trend in relation to the number of floors.

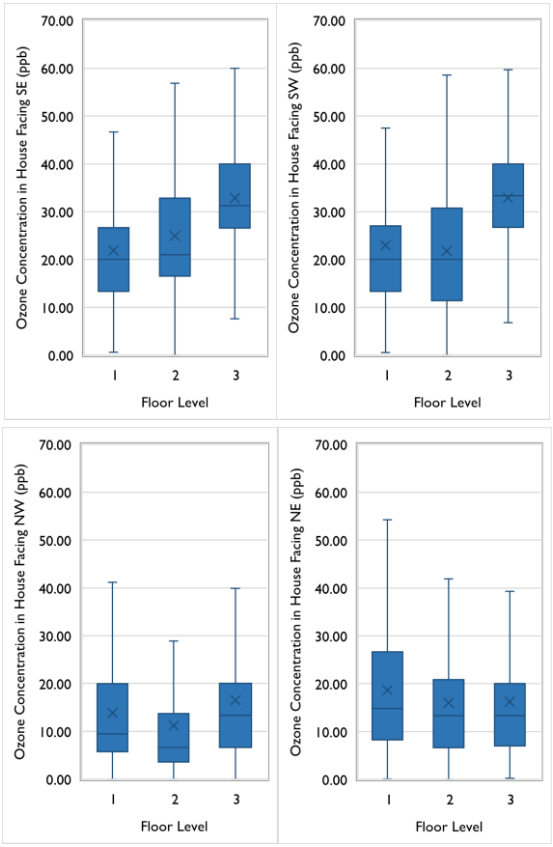

Figure 5: Indoor ozone concentration distribution on each floor in four orientations.

The results demonstrate that in houses facing south-east and south-west, the concentration of ozone increases as the number of floors increases. This can be attributed to the fact that ozone tends to disperse in lower areas and is less likely to accumulate in higher areas, resulting in higher concentrations on the upper floors. In contrast, for houses facing north-west and north-east, the highest ozone concentration was found on the first floor, with concentrations decreasing on the second and third floors. This trend can be explained by the typical behavior of ozone, which is primarily produced near ground level and then transported upward by convection and diffusion, leading to a higher concentration on the lower floors, while the upper floors exhibit lower concentrations.

Ozone exposures at different heights. Figure 6 presents the indoor ozone concentration distribution at different heights (1.0m, 1.5m, and 1.7m) per floor in four different orientations. Notably, houses facing south-east and south-west exhibited little variation in ozone concentration across the three heights. In contrast, houses facing north-west and north-east showed a slight decreasing trend in ozone concentration with increasing height. It is also worth noting that ozone concentrations at a height of 1.0m have the largest range, with values reaching up to an extremely unhealthy level of 62 ppb. This finding is particularly concerning as 1.0m is considered the breathing zone for children, suggesting that they could be at higher risk of experiencing health effects.

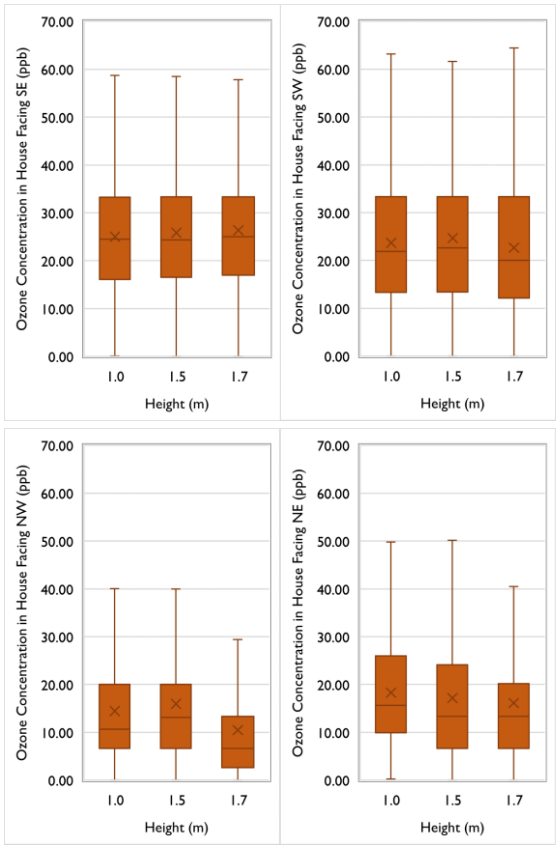

Figure 6: Indoor ozone concentration distribution at 1.0m, 1.5m, 1,7m height per floor in four orientations.

Correlation analysis. After conducting a correlation analysis, it was determined that house orientation has a positive correlation with indoor ozone concentration, although the correlation is not particularly strong (correlation coefficient $\rho = 0.25$). Houses facing south generally exhibit higher indoor ozone concentrations compared to those facing north. This can be attributed to increased sunlight on south-facing houses, which can result in the release of volatile organic compounds (VOCs) that react with ozone and increase its penetration probability getting indoors. This finding emphasizes the importance of considering house orientation during the design phase. Architects and builders should incorporate

https://doi.org/10.26868/25222708.2023.1472

an additional layer of consideration into their design process to address indoor ozone exposures effectively.

Moreover, upon closer examination of Figure 7, it is evident that the length-to-width ratio, or house geometry, exhibits a weak negative correlation with indoor ozone concentration (correlation coefficient ρ = -0.21). Specifically, houses with a higher length-to-width ratio are prone to have lower indoor ozone concentrations due to their linear and efficient shape, which facilitates improved air circulation and ventilation. The enhanced air circulation can dilute and disperse ozone, resulting in reduced indoor ozone concentrations. This finding implies that the design of building shape and geometry is also critical in minimizing exposure to ozone.

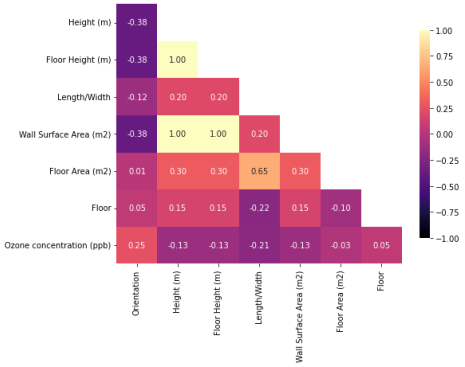

Figure 7: Heat map representation of the correlation matrix.

Discussion on the architectural strategies for indoor ozone pollution mitigation. Architectural strategies for mitigating indoor ozone pollution play a crucial role in residential environments where outdoor sources primarily contribute to indoor ozone levels. One of the most effective interventions is to minimize and reduce indoor ozone generation. To achieve this, architects can prioritize the utilization of low or no ozone-producing materials, such as low-VOC paints, formaldehyde-free insulation, and flooring made from natural materials when selecting building materials. By incorporating these measures into the design process, architects can contribute to creating healthier indoor environments with lower ozone levels.

Our study revealed that higher concentrations of ozone were observed on upper floors. To mitigate ozone concentrations on higher floors, architects can consider incorporating design strategies such as relatively smaller window sizes on upper floors to prevent outdoor ozone penetration through unintended airflows. In addition, proper building sealing techniques like air barriers, weatherstripping, and other sealing techniques, can be employed to prevent outdoor ozone from infiltrating the indoor environment. It's noteworthy that the existing building design guidelines provide limited information on how to integrate architectural strategies to help mitigate ozone pollution. Therefore, it's crucial for architects to receive comprehensive training and education to pay more attention to IAQ. This includes understanding proper ventilation practices, utilizing air purifiers, and selecting low-emission building materials to mitigate indoor ozone pollution.

Conclusion

Ozone is a well-known ambient air pollutant that poses acute and chronic health risks, with its concentrations positively correlated with temperature. These risks are expected to worsen as global warming continues. While studies have shown the significance of considering IAQ in building design, it has not received adequate attention in design objectives. Our research focused on studying the spatial distribution of ozone in typical rowhouses in one of the most ozone-polluted cities in the United States, utilizing experimentally validated CFD simulations.

The study conducted simulations on twelve rowhouses under climate change, and yielded several important findings. Firstly, houses facing south-east and south-west exhibited significantly higher mean ozone concentrations, likely influenced by prevailing winds and intense solar radiation. Additionally, higher floors had higher ozone concentrations due to ozone dispersion patterns. Indoor ozone exposure at a height of 1.0m was found to reach unhealthy levels of up to 62 ppb, raising particularly concerns for children's health. Furthermore, building geometry also played a role, with a higher length-to-width ratio correlating with lower indoor ozone concentrations.

To mitigate indoor ozone pollution in residential environments, architectural strategies should prioritize building geometry, orientation, window location and sizes, the use of low or no ozone-producing materials, and proper building sealing techniques. Overall, the implementation of these (passive) architectural strategies can enhance the resilience of housing against future ozone pollution events, while simultaneously promoting healthier and more sustainable living environments. Overall, our study highlights the importance of incorporating IAQ considerations into architectural design practices, especially in the context of rising ozone pollution levels associated with climate change.

Acknowledgement

The authors would like to express their gratitude to the participants who generously offered their homes for the field study. QZ's research received support from the China Scholarship Council. NM's research was supported by Worcester Polytechnic Institute under the Start-Up Grant.

References

Alizadeh, M., & Sadrameli, S. M. (2018). Numerical modeling and optimization of thermal comfort in building: Central composite design and CFD simulation. *Energy and Buildings 164*, 187–202.

American Lung Association. (2020). *The State of the Air 2020*.

Bell, M. L., Dominici, F., Ebisu, K., Zeger, S. L., & Samet, J. M. (2007). Spatial and temporal variation in PM2. 5 chemical composition in the United States for health effects studies. *Environmental Health Perspectives 115*(7), 989–995.

Ben-David, T., & Waring, M. S. (2016). Impact of natural versus mechanical ventilation on simulated indoor air quality and energy consumption in offices in fourteen U.S. cities. *Building and Environment 104*, 320–336.

Ben-David, T., & Waring, M. S. (2018). Interplay of ventilation and filtration: Differential analysis of cost function combining energy use and indoor exposure to PM2.5 and ozone. *Building and Environment 128*, 320–335.

Chang, H. H., Hao, H., & Sarnat, S. E. (2014). A statistical modeling framework for projecting future ambient ozone and its health impact due to climate change. *Atmospheric Environment 89*, 290–297.

Chen, C., Zhao, B., Zhou, W., Jiang, X., & Tan, Z. (2012). A methodology for predicting particle penetration factor through cracks of windows and doors for actual engineering application. *Building and Environment 47*, 339–348.

Cohen, A. J., Brauer, M., Burnett, R., Anderson, H. R., Frostad, J., Estep, K., Balakrishnan, K., Brunekreef, B., Dandona, L., Dandona, R., Feigin, V., Freedman, G., Hubbell, B., Jobling, A., Kan, H., Knibbs, L., Liu, Y., Martin, R., Morawska, L., … Forouzanfar, M. H. (2017). Estimates and 25-year trends of the global burden of disease attributable to ambient air pollution: An analysis of data from the Global Burden of Diseases Study 2015. *The Lancet 389*(10082), 1907–1918.

Dockery, D. W., & Evans, J. S. (2017). Tallying the bills of mortality from air pollution. *The Lancet 389*(10082), 1862–1864.

Hajdukiewicz, M., Geron, M., & Keane, M. M. (2013). Formal calibration methodology for CFD models of naturally ventilated indoor environments. *Building and Environment 59*, 290–302.

Jan, R., Roy, R., Yadav, S., & Satsangi, P. G. (2017). Exposure assessment of children to particulate matter and gaseous species in school environments of Pune, India. *Building and Environment 111*, 207–217.

Kamel, M. A., Elbanhawy, A. Y., & Abo El-Nasr, M. (2021). Quantification of deviations between grey-box and constant efficiency modeling and optimization of trigeneration systems using a data-driven RMSD indicator. *Sustainable Energy Technologies and Assessments 45*, 101195.

Klepeis, N. E., Nelson, W. C., Ott, W. R., Robinson, J. P., Tsang, A. M., Switzer, P., Behar, J. V., Hern, S. C., & Engelmann, W. H. (2001). The National Human Activity Pattern Survey (NHAPS): A resource for assessing exposure to environmental pollutants. *Journal of Exposure Science & Environmental Epidemiology 11*(3).

Lai, D., Karava, P., & Chen, Q. (2015). Study of outdoor ozone penetration into buildings through ventilation and infiltration. *Building and Environment 93*, 112–118.

Levy, J. I., Carrothers, T. J., Tuomisto, J. T., Hammitt, J. K., & Evans, J. S. (2001). Assessing the public health benefits of reduced ozone concentrations. *Environmental Health Perspectives 109*(12), 1215–1226.

Ma, N., Aviv, D., Guo, H., & Braham, W. W. (2021). Measuring the right factors: A review of variables and models for thermal comfort and indoor air quality. *Renewable and Sustainable Energy Reviews 135*, 110436.

Ma, N., Hakkarainen, M., Hou, M., Aviv, D., & Braham, W. W. (2022). Impacts of building envelope design on indoor ozone exposures and health risks in urban environments. *Indoor and Built Environment*, 1420326X221112010.

Ma, N., Zhang, Q., Murai, F., Braham, W. W., & Samuelson, H. W. (2023). Learning building occupants' indoor environmental quality complaints and dissatisfaction from text-mining Booking.com reviews in the United States. *Building and Environment 237*, 110319.

Mackay, R. M., & Probert, S. D. (2000). Enhancing the designs and impacts of guides for achieving reduced energy-consumptions. *Applied Energy 66*(1), 1–50.

Mudway, I. S., & Kelly, F. J. (2000). Ozone and the lung: A sensitive issue. *Molecular Aspects of Medicine 21*(1–2), 1–48.

Schade, R. S., & Architects, B. (2008). Philadelphia rowhouse manual. *City of Philadelphia.*

Sloan Brittain, O., Wood, H., & Kumar, P. (2021). Prioritising indoor air quality in building design can mitigate future airborne viral outbreaks. *Cities & Health 5*(sup1), S162–S165.

Sundell, J., Levin, H., Nazaroff, W. W., Cain, W. S., Fisk, W. J., Grimsrud, D. T., Gyntelberg, F., Li, Y., Persily, A. K., Pickering, A. C., Samet, J. M., Spengler, J. D., Taylor, S. T., & Weschler, C. J. (2011a). Ventilation rates and health: Multidisciplinary review of the scientific literature. *Indoor Air 21*(3), 191–204.

Sundell, J., Levin, H., Nazaroff, W. W., Cain, W. S., Fisk, W. J., Grimsrud, D. T., Gyntelberg, F., Li, Y., Persily, A. K., Pickering, A. C., Samet, J. M., Spengler, J. D., Taylor, S. T., & Weschler, C. J. (2011b). Ventilation rates and health: Multidisciplinary review of the scientific literature. *Indoor Air 21*(3), 191–204.

Walker, I. S., & Sherman, M. H. (2013). Effect of ventilation strategies on residential ozone levels. *Building and Environment 59*, 456–465.

Wei, W., Ramalho, O., & Mandin, C. (2015). Indoor air quality requirements in green building certifications. *Building and Environment 92*, 10–19.

Weschler, C. J. (2000). Ozone in indoor environments: Concentration and chemistry. *Indoor Air 10*(4), 269–288.

Westervelt, D. M., Horowitz, L. W., Naik, V., Tai, A. P. K., Fiore, A. M., & Mauzerall, D. L. (2016). Quantifying PM2.5-meteorology sensitivities in a global climate model. *Atmospheric Environment 142*, 43–56.

Wong, I. L. (2017). A review of daylighting design and implementation in buildings. *Renewable and Sustainable Energy Reviews 74*, 959–968.

World Health Organization. (2021). *WHO global air quality guidelines: Particulate matter (PM2.5 and PM10), ozone, nitrogen dioxide, sulfur dioxide and carbon monoxide*.

Xu, Y., Li, F., & Asgari, A. (2022). Prediction and optimization of heating and cooling loads in a residential building based on multi-layer perceptron neural network and different optimization algorithms. *Energy 240*, 122692.

Yang, J., & Zhao, Y. (2023). Performance and application of air quality models on ozone simulation in China – A review. *Atmospheric Environment 293*, 119446.